

This is the accepted manuscript made available via CHORUS. The article has been published as:

# Triaxial projected shell model study of the rapid changes in $B(E2)$ for $^{180-190}\text{Pt}$ isotopes

G. H. Bhat, J. A. Sheikh, Y. Sun, and U. Garg

Phys. Rev. C **86**, 047307 — Published 19 October 2012

DOI: [10.1103/PhysRevC.86.047307](https://doi.org/10.1103/PhysRevC.86.047307)

# Triaxial projected shell model study of the rapid changes in $B(E2)$ for $^{180-190}\text{Pt}$ isotopes

G. H. Bhat<sup>1</sup>, J. A. Sheikh<sup>1,2</sup>, Y. Sun<sup>3,4,2\*</sup>, U. Garg<sup>5</sup>

<sup>1</sup> Department of Physics, University of Kashmir, Srinagar 190 006, India

<sup>2</sup> Department of Physics and Astronomy, University of Tennessee, Knoxville, TN 37996, USA

<sup>3</sup> Department of Physics, Shanghai Jiao Tong University, Shanghai 200240, People's Republic of China

<sup>4</sup> Institute of Modern Physics, Chinese Academy of Sciences, Lanzhou 730000, People's Republic of China

<sup>5</sup> Department of Physics, University of Notre Dame, Notre Dame, IN 46556, USA

The mass region with proton number just below the magic number  $Z = 82$  is known to exhibit a rich variety of shape phenomena. Inspired by the recent extensive experimental measurements of the transition probabilities for the yrast bands in some Pt-isotopes in this mass region, we have performed a detailed investigation of  $^{180-190}\text{Pt}$  using the triaxial projected shell model approach (TPSM). It is demonstrated that by performing the exact three-dimensional angular-momentum-projection on multi-quasiparticle configurations, constructed from the triaxially-deformed mean-field, the TPSM provides a consistent description of the yrast band structures,  $\gamma$ -vibrational, and second  $0^+$  band in these nuclei. Further, the observed rapid variations in the quadrupole transition probability along the yrast line of these isotopes are well reproduced in the present study.

PACS numbers: 21.60.Cs, 23.20.Lv, 23.20.-g, 27.70.+q

The study of nuclear shape changes as a function of particle-number, angular-momentum, and excitation energy has been one of the important research areas in nuclear structure physics. In particular, in the vicinity of the proton shell closure with  $Z = 82$ , rapid variations of the nuclear shape have been extensively studied [1]. In the lighter Pb-isotopes, one low-lying excited  $0^+$  state has been observed in all the even-even isotopes from  $A = 184$  to  $204$  [2–4]. In  $^{186}\text{Pb}$  [5] and  $^{188}\text{Pb}$  [6], two excited  $0^+$  states have been observed and the hindrance factors for the three  $\alpha$ -branches from  $^{190}\text{Po}$  and  $^{192}\text{Po}$  support the picture where the three shape minima of prolate, oblate and spherical coexist within a narrow range of energy. The Hg-isotopes also display a broad variety of nuclear shapes [7–12]. In light Hg-isotopes, two distinct minima are associated with weakly deformed oblate and well deformed prolate deformations. For moderate spins, bands coexist with non-collective prolate shape in some Hg-isotopes [13] and at high spins superdeformed states are populated [14, 15].

Interesting features on collective motion are known to occur in Pt-isotopes as well [16–23]. The co-existence between prolate and oblate shapes has been invoked to interpret the yrast band-structures and transition probabilities [16–18] for these isotopes. There has been considerable effort to study nuclear structure properties in Pt-isotopes using both heavy-ion [19–22] and Coulomb excitation experiments [23]. Very recently, detailed lifetime measurements of the yrast bands have been performed [24, 25] for  $^{182,186}\text{Pt}$  isotopes and it has been shown that a steep increase in  $B(E2)$  transition probabilities can partially be explained by using the prescription of mixing of two bands corresponding to two different shapes [24]. Detailed theoretical investigation of the ground-state deformations of Pt-isotopes from  $A = 166$  to  $204$  has been carried out using the D1S, D1N, and D1M parameterizations of the Gogny energy density functional approach [26]. It is evident from figure 1 in

Ref. [26] that in the axial limit, a sudden transition from prolate to oblate shape is predicted around  $A = 188$ , in agreement with the results obtained using the Skyrme density functional [28] and the relativistic mean-field approach [29]. However, in a more generalized treatment with broken axial symmetry, also performed in Ref. [26, 27], it is evident that potential energy surfaces evolve from prolate shape in the lighter isotopes with  $A = 166 - 182$ , to triaxial shape or  $\gamma$ -soft for intermediate isotopes with  $A = 184 - 196$ , and to oblate shapes for the neutron-rich isotopes. These results are independent of the parameterization employed in the Gogny density functional approach. The theoretical work, therefore, suggests that from  $A = 184$  to  $196$ , Pt-isotopes should be studied by using the triaxial mean-field approach. Indeed, the early systematic study of electromagnetic transition properties using the axially-symmetric mean-field as a starting point indicated a clear deficiency in the wave functions for the description of  $^{184-196}\text{Pt}$  isotopes [30].

The purpose of the present work is to investigate systematically the band structures and transition probabilities of the  $^{180-190}\text{Pt}$ -isotopes using the triaxial projected shell model approach (TPSM) [31]. In this model, three-dimensional angular-momentum projection technique is employed to project out the good angular-momentum states from the triaxially-deformed Slater determinant. This approach opens up opportunities to treat problems that otherwise are difficult to interpret in the axial-symmetry limit. For example, TPSM approach has more recently been used to investigate the interplay between the vibrational and the quasi-particle excitation modes in  $^{166-172}\text{Er}$  [32]. It has been established that a low-lying  $K = 3$  bands observed in these nuclei are, in fact, built on triaxially-deformed two-quasiparticle states. This band is observed to interact with the  $\gamma$ -vibrational band and becomes favoured at high angular-momentum for some Er-nuclei.

Further, it is important to note that  $^{180-190}\text{Pt}$ -isotopes have well developed low-lying  $\gamma$ -vibrational bands that can be described naturally when triaxial degree of freedom is introduced in the mean-field [33]. In the axial-symmetry limit,

---

\*Corresponding author at SJTU: sunyang@sjtu.edu.cn

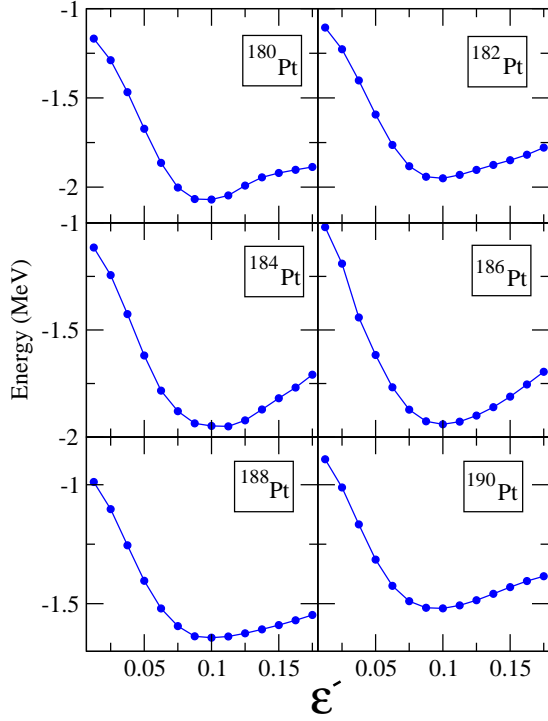


FIG. 1: (Color online) Variation of the projected energy surfaces of the ground state as a function of triaxiality  $\epsilon'$  for  $^{180-190}\text{Pt}$ .

TABLE I: The axial deformation parameter  $\epsilon$  and triaxial deformation parameter  $\epsilon'$  employed in the calculation for  $^{180-190}\text{Pt}$ .

	$^{180}\text{Pt}$	$^{182}\text{Pt}$	$^{184}\text{Pt}$	$^{186}\text{Pt}$	$^{188}\text{Pt}$	$^{190}\text{Pt}$
$\epsilon$	0.256	0.220	0.218	0.225	0.158	0.128
$\epsilon'$	0.100	0.100	0.110	0.100	0.095	0.090

$\gamma$ -vibrational bands don't appear in our model and is the reason that we have also performed TPSM study of  $^{180,182}\text{Pt}$  as these isotopes have well developed  $\gamma$ -bands.

The TPSM approach has been already discussed in our earlier studies [34–38], and we shall only mention that its basic philosophy is the same as that followed in the standard shell model approach with the only difference in that a deformed basis space is employed rather than a spherical. The basis is constructed by solving the triaxially-deformed mean-field Nilsson Hamiltonian. Such a deformed basis is projected to good angular-momentum states by using the explicit three-dimensional projection technique [39, 40]. These projected states are then used to diagonalize the effective shell model Hamiltonian consisting of the Pairing plus Quadrupole-Quadrupole interaction. Although this effective interaction is quite simple as compared to Skyrme, Gogny, or that in relativistic approaches, it has the advantage that it allows to perform a systematic analysis of high-spin band structures of a long series of isotopic chains with a minimal computational effort. Further, in the TPSM study of even-even isotopes, projection is performed from zero-, two- and four-quasiparticle states and configuration mixing is carried out with such multi-quasiparticle configurations. The later point is known to be

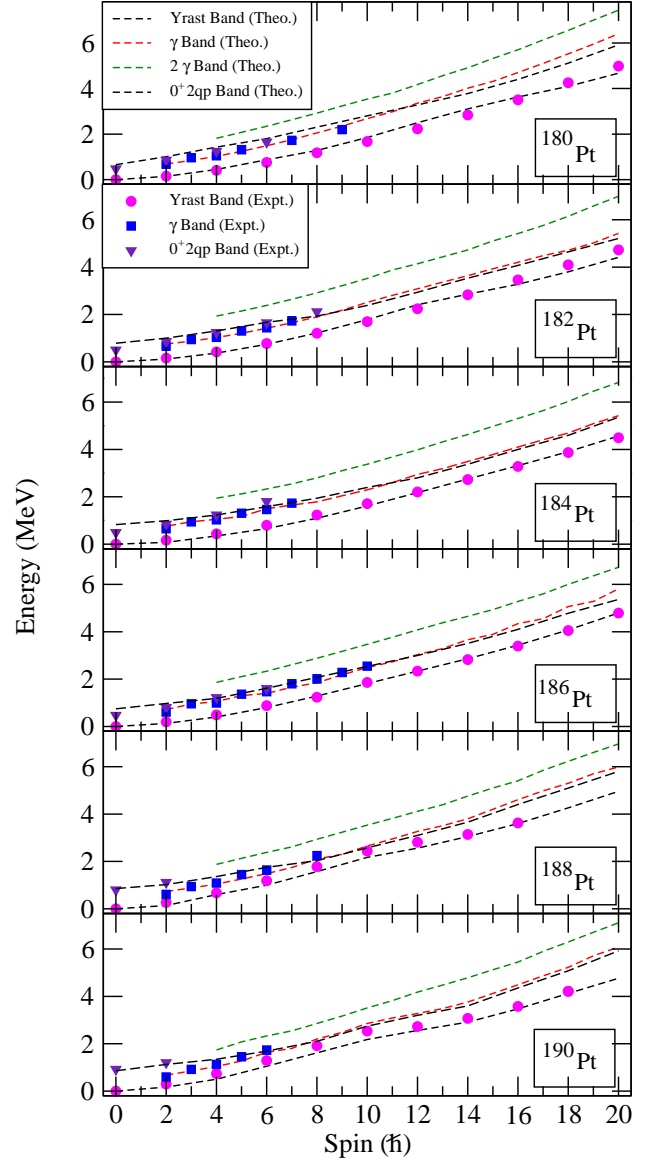


FIG. 2: (Color online) Comparison of the TPSM energies after configuration mixing with the available experimental data for  $^{180-190}\text{Pt}$ . Data are taken from [47–51].

crucial in understanding many structural phenomena. In contrast, in most of the “so-called” beyond-mean-field study using density functional approaches [41–45], projection is restricted to zero-quasiparticle configuration only.

In the present work, the Nilsson potential has been solved for the  $^{180-190}\text{Pt}$  isotopes with the deformation parameters listed in Table I. The axial deformation parameters,  $\epsilon$ , have been chosen by varying the tabulated values given in Ref. [46] such that the measured value of  $B(E2, 2^+ \rightarrow 0^+)$  transition is described reasonably. This re-adjustment of the tabulated values is required as the nuclear model employed in the present analysis is different from that used in Ref. [46]. The non-axial deformations,  $\epsilon'$ , are chosen in such a way that the bandhead of the  $\gamma$ -bands is reproduced. These non-axial deformations

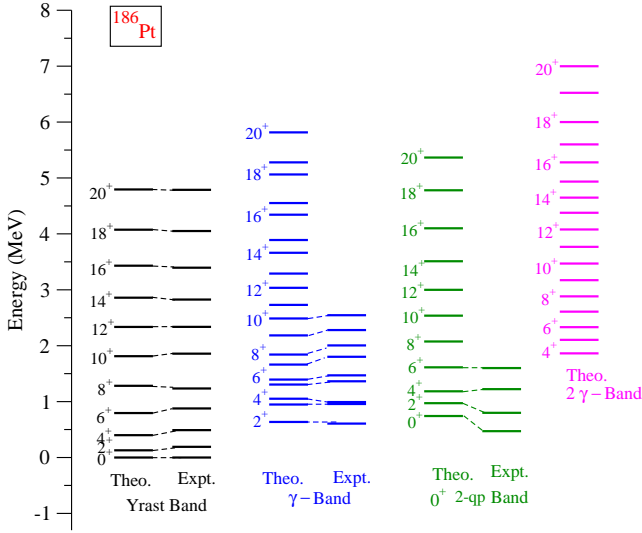


FIG. 3: (Color online) Comparison of the calculated energy levels with the available experimental data for  $^{186}\text{Pt}$ . Data are taken from [49].

are consistent with the values obtained from the minimum of the potential energy surfaces shown in Fig. 1. In this figure, projected ground-state energy is drawn as a function of the triaxial parameter with axial deformation parameter held fixed. It needs to be emphasised that these deformation parameters are used to solve the triaxial potential from which the deformed basis space of the TPMS is constructed. In principle, results of shell-model-type calculations should be independent of the deformation used in constructing the basis. However, in practice, as limited basis space is employed, the final results become dependent on the basis deformation. It is, therefore, important to choose optimum deformations to start with. The pairing interaction parameters employed in the present work are same as those used in our recent work on Er-isotopes [32].

In the second stage of the TPMS study, the projected states are then employed as a new basis for diagonalization of the shell model Hamiltonian. In the diagonalization process, the number of projected states employed is nearly 40 for all nuclei studied in the present work. Fig. 2 depicts the calculated bands after diagonalization and also displays the corresponding available experimental data. It is important to point out that, although the calculated bands in Fig. 2 are labeled as  $\gamma$ -,  $\gamma\gamma$ -, and excited  $K = 0^+$ -bands, these are only the dominant components in the wavefunction.

In general, it is quite evident from Fig. 2 that agreement between the TPMS results and the experimental data is quite satisfactory. The crossing of the excited  $0^+$  band with the  $\gamma$ -band is noted to occur at about  $I = 8$  for all the Pt-isotopes. Unfortunately, only few low-lying states of the excited  $0^+$  band are experimentally known and it is not possible to corroborate this prediction. For a more detailed comparison of the TPMS results with the experimental data, level energies of  $^{186}\text{Pt}$  are plotted in Fig. 3 as an example. The known experimental levels are well described, and the observed levels of the  $\gamma$ -band

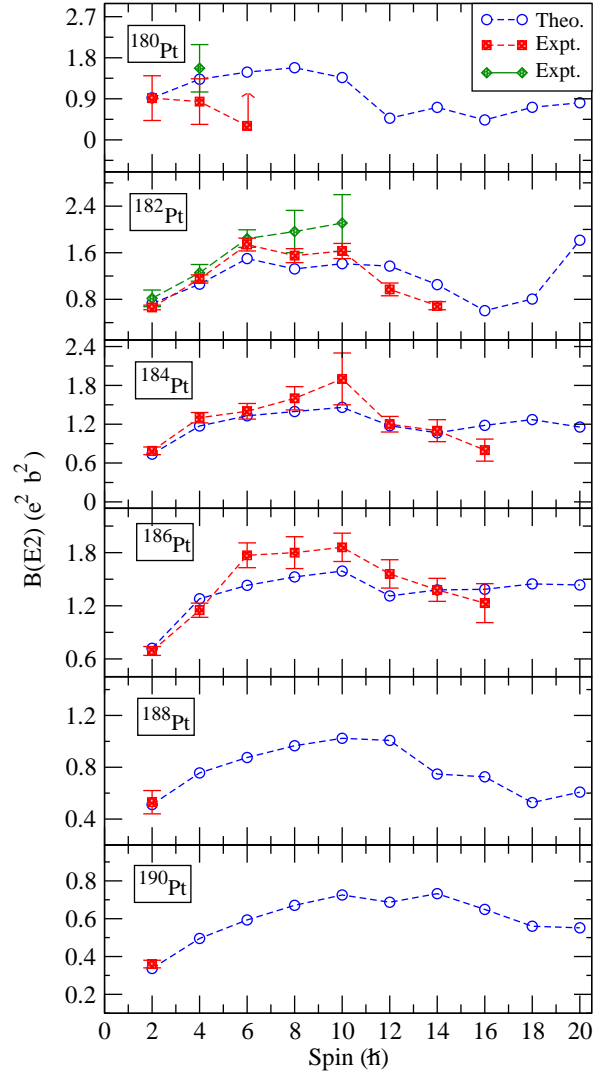


FIG. 4: (Color online) Detailed comparison of the calculated  $B(E2)$ 's in  $^{180-190}\text{Pt}$  with experimental data [20, 24, 25, 47–51]. There are two sets of experimental data for  $^{182}\text{Pt}$  - one from Ref. [24] (shown in red colour) and the other from Ref. [25] (shown in green colour). The  $4^+$  transition in  $^{180}\text{Pt}$  (shown in green colour) is from Ref. [19] and is almost a factor of two larger than given in Ref. [20] (shown in red colour).

are also well reproduced.

The major emphasis of the present work is to elucidate the recent measurement of the lifetimes of the studied Pt-isotopes along the yrast line. The data depicts a rapid variation of the  $B(E2)$  transition probabilities along the yrast band with probabilities showing increasing trend for low-spin and dropping for high-spin states. We have evaluated the transition probabilities of the Pt-isotopes using the wavefunctions of the TPMS analysis. The expressions and other details for the evaluation of transition probability are discussed in our previous works [37, 38] and in the present study we shall only present the results. For  $B(E2)$  calculations, standard effective charges,  $1.5e$  for protons and  $0.5e$  for neutrons, are employed as in our recent work on even-even Er-isotopes [32].

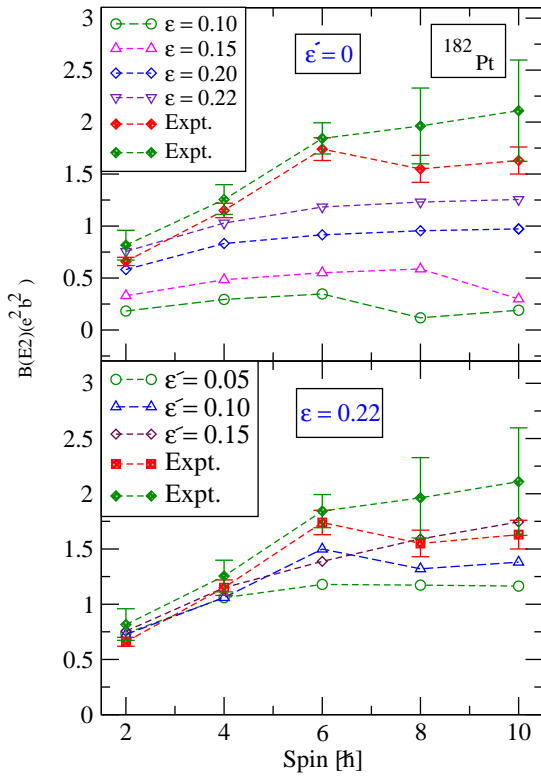


FIG. 5: (Color online) Behavior of the  $B(E2)$ 's of various configurations as a function of axial and triaxial deformations for  $^{182}\text{Pt}$ . In the upper panel, the  $B(E2)$ 's have been evaluated for a fixed value of  $\varepsilon' = 0.0$  and in the lower panel  $\varepsilon = 0.22$  has been chosen. There are two sets of experimental data - one from Ref. [24] (shown in red colour) and the other from Ref. [25] (shown in green colour).

In Fig. 4, the calculated  $B(E2)$  transition probabilities are compared with the known experimental values. It is quite evident from the figure that the transition probabilities are well reproduced by the TPSM approach. In particular, the increasing trend of  $B(E2)$  for low-spin states and the drop for high-spin states is well described by the calculations. The decreasing trend at high-spin can be traced to the crossing of the 2-qp neutron configuration with the ground-state band. It is known, in majority of deformed rare-earth nuclei, that the bands built on high- $j$  unnatural parity orbitals (neutrons in  $1i_{13/2}$ ; protons in  $1h_{11/2}$ ) cross the ground-state band in the spin-regime  $I = 8 - 16$ . The transition probabilities in the band-crossing region are reduced as these are evaluated between predomi-

nantly ground-state and two-quasiparticle aligned configurations.

In order to understand the mechanism behind the increase of  $B(E2)$  for lower spin values, we have calculated transition probabilities with varying  $\varepsilon$  and  $\varepsilon'$  and the results are presented in Fig. 5. In the upper panel of the figure, the results are displayed for the axial symmetry case by taking  $\varepsilon' = 0$ , and varying  $\varepsilon$  to see the deformation dependence. It is evident from the upper panel that the calculated  $B(E2)$  values increase with increasing axial deformation, and the optimum deformation of  $\varepsilon = 0.22$  reproduces the first two data points in  $B(E2)$  transition probabilities. However, none of the calculations with an axial deformation only can describe the rapid increase of  $B(E2)$  for spin value of  $I = 6$ . In the lower panel of Fig. 5, calculations for a fixed  $\varepsilon = 0.22$  and varying triaxiality  $\varepsilon'$  are presented. The onset of triaxiality in the deformed basis now increases the  $B(E2)$  values for  $I = 6$ , thus correctly describing the observed variation trend with increasing spin. Therefore, present calculations provide an alternative to the band-mixing explanation, offered previously, to describe the observed  $B(E2)$  behaviour.

In summary, in the present work, we have firstly demonstrated that high-spin band-structures of the studied Pt-isotopes are reproduced quite well in the TPSM approach. In particular, the yrast- and  $\gamma$ -bands are described quite satisfactorily. It has been shown that the observed excited  $0^+$  band has a two-quasiparticle proton structure. The bandhead of this excited band is reasonably well reproduced. Secondly, we have evaluated the  $B(E2)$  transition probabilities along the yrast line that has been the major spotlight of the present investigation. It has been noted that the TPSM approach provides an accurate description of the measured  $B(E2)$ . In particular, we have shown that both axial and non-axial deformation contribute to the observed behavior of the  $B(E2)$  in the low-spin regime. In the high-spin region, it has been substantiated that the drop in the transitions is due to the rotational alignment of neutrons.

One of us (U.G.) thanks colleagues of Department of Physics for the hospitality extended to him when he visited Shanghai Jiao Tong University (SJTU). Research at SJTU was partially supported by the National Natural Science Foundation of China (Nos. 11135005 and 11075103) and the 973 Program of China (No. 2013CB834401), and at the University of Notre Dame by the U.S. National Science Foundation (Grant No. PHY-1068192).

- 
- [1] K. Heyde and J. L. Wood, *Rev. Mod. Phys.* **83**, 1467 (2011).
  - [2] P. Van Duppen, E. Coenen, K. Deneffe, M. Huyse, K. Heyde, and P. Van Isacker, *Phys. Rev. Lett.* **52**, 1974 (1984).
  - [3] P. Van Duppen, E. Coenen, K. Deneffe, M. Huyse, and J. L. Wood, *Phys. Rev. C* **35**, 1861 (1987).
  - [4] M. Bender, P. Bonche, T. Duguet, and P.-H. Heenen, *Phys. Rev. C* **69**, 064303 (2004).
  - [5] A. N. Andreyev, M. Huyse, P. Van Duppen, L. Weissman, D.

- Ackermann, J. Gerl, F. Hessberger, S. Hofmann, A. Kleinbühl, G. Münzenberg, S. Reshitko, C. Schlegel, H. Schaffner, P. Cagarda, M. Matos, S. Saro, A. Keenan, C. J. Moore, C. D. O'Leary, R. D. Page, M. J. Taylor, H. Kettunen, M. Leino, A. Lavrentiev, R. Wyss, and K. Heyde, *Nucl. Phys. A* **682**, 482c (2001).
- [6] R. D. Page, R. G. Allatt, T. Enqvist, K. Eskola, P. T. Greenlees, P. Jones, R. Julin, P. Kuusiniemi, M. Leino, W. H. Trzaska, and

- J. Uusitalo, *J. Phys. G: Nucl. Part. Phys.* **25**, 771 (1999).
- [7] R. D. Page, A. N. Andreyev, D. R. Wiseman, P. A. Butler, T. Grahn, P. T. Greenlees, R.-D. Herzberg, M. Huyse, G. D. Jones, P. M. Jones, D. T. Joss, R. Julin, S. Juutinen, H. Kankaanpää, A. Keenan, H. Kettunen, P. Kuusiniemi, M. Leino, M. Muikku, P. Nieminen, P. Rahkila, G. I. Rainovski, C. Scholey, J. Uusitalo, K. Van de Vel, and P. Van Duppen, *Phys. Rev. C* **84**, 034308 (2011).
- [8] J. Elseviers, A. N. Andreyev, S. Antalic, A. Barzakh, N. Bree, T. E. Cocolios, V. F. Comas, J. Diriken, D. Fedorov, V. N. Fedosseyev, S. Franchoo, J. A. Heredia, M. Huyse, O. Ivanov, U. Köster, B. A. Marsh, R. D. Page, N. Patronis, M. Seliverstov, I. Tsekhanovich, P. Van den Bergh, J. Van De Walle, P. Van Duppen, M. Venhart, S. Vermote, M. Veselský, and C. Wagemans, *Phys. Rev. C* **84**, 034307 (2011).
- [9] M. Scheck, T. Grahn, A. Petts, P. A. Butler, A. Dewald, L. P. Gaffney, M. B. Gómez Hornillos, A. Görgen, P. T. Greenlees, K. Helariutta, J. Jolie, P. Jones, R. Julin, S. Juutinen, S. Ketelhut, T. Kröll, R. Krücken, M. Leino, J. Ljungvall, P. Maierbeck, B. Melon, M. Nyman, R. D. Page, J. Pakarinen, E. S. Paul, Th. Pissulla, P. Rahkila, J. Sarén, C. Scholey, A. Semchenkov, J. Sorri, J. Uusitalo, R. Wadsworth, and M. Zielińska, *Phys. Rev. C* **81**, 014310 (2010).
- [10] M. Scheck, P. A. Butler, L. P. Gaffney, N. Bree, R. J. Carroll, D. Cox, T. Grahn, P. T. Greenlees, K. Hauschild, A. Herzan, M. Huyse, U. Jakobsson, P. Jones, D. T. Joss, R. Julin, S. Juutinen, S. Ketelhut, R.-D. Herzberg, M. Kowalczyk, A. C. Larsen, M. Leino, A. Lopez-Martens, P. Nieminen, R. D. Page, J. Pakarinen, P. Papadakis, P. Peura, P. Rahkila, S. Rinta-Antila, P. Ruotsalainen, M. Sandzelius, J. Saren, C. Scholey, J. Sorri, J. Srebrny, P. Van Duppen, H. V. Watkins, and J. Uusitalo, *Phys. Rev. C* **83**, 037303 (2011).
- [11] M. Sandzelius, E. Ganioglu, B. Cederwall, B. Hadinia, K. Andgren, T. Bäck, T. Grahn, P. Greenlees, U. Jakobsson, A. Johnson, P. M. Jones, R. Julin, S. Juutinen, S. Ketelhut, A. Khaplanov, M. Leino, M. Nyman, P. Peura, P. Rahkila, J. Sarén, C. Scholey, J. Uusitalo, and R. Wyss, *Phys. Rev. C* **79**, 064315 (2009).
- [12] T. Grahn, A. Petts, M. Scheck, P. A. Butler, A. Dewald, M. B. Gómez Hornillos, P. T. Greenlees, A. Görgen, K. Helariutta, J. Jolie, P. Jones, R. Julin, S. Juutinen, S. Ketelhut, R. Krücken, T. Kröll, M. Leino, J. Ljungvall, P. Maierbeck, B. Melon, M. Nyman, R. D. Page, Th. Pissulla, P. Rahkila, J. Sarén, C. Scholey, A. Semchenkov, J. Sorri, J. Uusitalo, R. Wadsworth, and M. Zieliska, *Phys. Rev. C* **80**, 014324 (2009).
- [13] F. G. Kondev, M. P. Carpenter, R. V. F. Janssens, I. Wiedenhöver, M. Alcorta, P. Bhattacharyya, L. T. Brown, C. N. Davids, S. M. Fischer, T. L. Khoo, T. Lauritsen, C. J. Lister, R. Nouicer, W. Reviol, L. L. Riedinger, D. Seweryniak, S. Siem, A. A. Sonzogni, J. Uusitalo, and P. J. Woods, *Phys. Rev. C* **61**, 011303(R) (1999).
- [14] D. Ye, R. V. F. Janssens, M. P. Carpenter, E. F. Moore, I. Ahmad, K. B. Beard, Ph. Benet, M. W. Drigert, U. Garg, Z. W. Grabowski, T. L. Khoo, F. L. H. Wolfs, T. Bengtsson, I. Ragnarsson, *Phys. Lett. B* **236**, 7 (1990).
- [15] R. V. F. Janssens and T. L. Khoo, *Annu. Rev. Nucl. Part. Sci.* **41**, 321 (1991).
- [16] P. M. Davidson, G. D. Dracoulis, T. Kibédi, A. P. Byrne, S. S. Andersson, A. M. Baxter, B. Fabricius, G. J. Lane, A. E. Stuchbery, *Nucl. Phys. A* **657**, 219 (1999).
- [17] F. G. Kondev, M. P. Carpenter, R. V. F. Janssens, I. Wiedenhöver, M. Alcorta, L. T. Brown, C. N. Davids, T. L. Khoo, T. Lauritsen, C. J. Lister, D. Seweryniak, S. Siem, A. A. Sonzogni, J. Uusitalo, P. Bhattacharyya, S. M. Fischer, W. Reviol, L. L. Riedinger, and R. Nouicer, *Phys. Rev. C* **61**, 044323 (2000).
- [18] D. G. Popescu, J. C. Waddington, J. A. Cameron, J. K. Johansson, and N. C. Schmeing, W. Schmitz, M. P. Carpenter, V. P. Janzen, J. Nyberg, and L. L. Riedinger, H. Hubel, G. Kajrys, S. Monaro, and S. Pilotte, C. Bourgeois, N. Perrin, H. Sergolle, D. Hojman, and A. Korichi, *Phys. Rev. C* **55**, 1175 (1997).
- [19] E. Williams, C. Plettner, E. A. McCutchan, H. Levine, N. V. Zamfir, R. B. Cakirli, R. F. Casten, H. Ai, C. W. Beausang, G. Gürdal, A. Heinz, J. Qian, D. A. Meyer, N. Pietralla, and V. Werner, *Phys. Rev. C* **74**, 024302 (2006).
- [20] M. J. A. de Voigt, R. Kaczarowski, H. J. Riezebos, R. F. Noorman, J. C. Bacelar, M. A. Deleplanque, R. M. Diamond, F. S. Stephens, J. Sauvage, and B. Roussi  re, *Nucl. Phys. A* **507**, 472 (1990).
- [21] Y. Oktem, D. L. Balabanski, B. Akkus, C. W. Beausang, M. Bostan, R. B. Cakirli, R. F. Casten, M. Danchev, M. Djongolov, M. N. Erduran, S. Erturk, K. A. Gladniski, G. Gürdal, J. Tm. Goon, D. J. Hartley, A. A. Hecht, R. Kr  cken, N. Nikolov, J. R. Novak, G. Rainovski, L. L. Riedinger, I. Yigitoglu, N. V. Zamfir, and O. Zeidan, *Phys. Rev. C* **76**, 044315 (2007).
- [22] E. A. McCutchan, R. F. Casten, V. Werner, R. Winkler, R. B. Cakirli, G. Gürdal, X. Liang, and E. Williams, *Phys. Rev. C* **78**, 014320 (2008).
- [23] C. Y. Wu, D. Cline, T. Czosnyka, A. Backlin, C. Baktash, R. M. Diamond, G. D. Dracoulis, L. Hasselgren, H. Kluge, B. Kotlinski, J. R. Leigh, J. O. Newton, W. R. Philips, S. H. Sie, J. Srebrny, and F. S. Stephens, *Nucl. Phys. A* **607**, 178 (1996).
- [24] J. C. Walpe, U. Garg, S. Naguleswaran, J. Wei, W. Reviol, I. Ahmad, M. P. Carpenter, and T. L. Khoo, *Phys. Rev. C* **85**, 057302 (2012).
- [25] K. A. Gladniski, P. Petkova, A. Dewald, C. Fransen, M. Hackstein, J. Jolie, Th. Pissulla, W. Rother, K. O. Zell, *Nucl. Phys. A* **877**, 19 (2012).
- [26] R. Rodr  guez-Guzm  n, P. Sarriguren, L. M. Robledo, and J. E. Garcia-Ramos, *Phys. Rev. C* **81**, 024310 (2010).
- [27] T. Nik   i  , D. Vretenar, and P. Ring, *Prog. Part. Nucl. Phys.* **66**, 519 (2011).
- [28] P. Sarriguren, R. Rodr  guez-Guzm  n, and L. M. Robledo, *Phys. Rev. C* **77**, 064322 (2008).
- [29] M. M. Sharma and P. Ring, *Phys. Rev. C* **46**, 1715 (1992).
- [30] B.-A. Bian, Y.-M. Di, G.-L. Long, Y. Sun, J.-y. Zhang, and J. A. Sheikh, *Phys. Rev. C* **75**, 014312 (2007).
- [31] J. A. Sheikh and K. Hara, *Phys. Rev. Lett.* **82**, 3968 (1999).
- [32] J. A. Sheikh, G. H. Bhat, Y.-X. Liu, F.-Q. Chen, and Y. Sun, *Phys. Rev. C* **84**, 054314 (2011).
- [33] Y. Sun, K. Hara, J. A. Sheikh, J. G. Hirsch, V. Velazquez, and M. Guidry, *Phys. Rev. C* **61**, 064323 (2000).
- [34] J. A. Sheikh, G. H. Bhat, Y. Sun, G. B. Vakil, and R. Palit, *Phys. Rev. C* **77**, 034313 (2008).
- [35] J. A. Sheikh, G. H. Bhat, R. Palit, Z. Naik, and Y. Sun, *Nucl. Phys. A* **824**, 58 (2009).
- [36] J. A. Sheikh, G. H. Bhat, Y. Sun, and R. Palit, *Phys. Lett. B* **688**, 305 (2010).
- [37] J. A. Sheikh, Y. Sun, and R. Palit, *Phys. Lett. B* **507**, 115 (2001).
- [38] G. H. Bhat, J. A. Sheikh, R. Palit, *Phys. Lett. B* **707**, 250 (2012).
- [39] K. Hara and S. Iwasaki, *Nucl. Phys. A* **332**, 61 (1979).
- [40] K. Hara and S. Iwasaki, *Nucl. Phys. A* **348**, 200 (1980).
- [41] M. Bender and P.-H. Heenen, *Phys. Rev. C* **78**, 024309 (2008).
- [42] T. R. Rodr  guez and J. L. Egido, *Phys. Rev. C* **81**, 064323 (2010).
- [43] J. M. Yao, J. Meng, P. Ring, and D. Pena Arteaga, *Phys. Rev. C* **79**, 044312 (2009).
- [44] K. Nomura, T. Otsuka, R. Rodr  guez-Guzm  n, L. M. Robledo, and P. Sarriguren, *Phys. Rev. C* **84**, 054316 (2011).

- [45] K. Nomura, T. Nikšić, T. Otsuka, N. Shimizu, and D. Vretenar, Phys. Rev. C **84**, 014302 (2011).
- [46] P. Möller, J.R. Nix, At. Data Nucl. Data Tables **59**, 185 (1995).
- [47] B. Singh and R. B. Firestone, Nucl. Data Sheets, **74**, 383 (1995).
- [48] C. M. Baglin, Nucl. Data Sheets, **111**, 275 (2010).
- [49] C. M. Baglin, Nucl. Data Sheets, **99**, 1 (2003).
- [50] B. Singh, Nucl. Data Sheets, **95**, 387 (2002).
- [51] B. Singh, Nucl. Data Sheets, **61**, 243 (1990).